Stabilized bubbles in the body: pressure-radius relationships and the limits to stabilization

HUGH D. VAN LIEW AND SOUMYA RAYCHAUDHURI
Department of Physiology, University at Buffalo, State University of New York, Buffalo, New York 14214

Van Liew, Hugh D., and Soumya Raychaudhuri. Stabilized bubbles in the body: pressure-radius relationships and the limits to stabilization. *J. Appl. Physiol.* 82(6): 2045–2053, 1997.—We previously outlined the fundamental principles that govern behavior of stabilized bubbles, such as the microbubbles being put forward as ultrasound contrast agents. Our present goals are to develop the idea that there are limits to the stabilization and to provide a conceptual framework for comparison of bubbles stabilized by different mechanisms. Gases diffuse in or out of stabilized bubbles in a limited and reversible manner in response to changes in the environment, but strong growth influences will cause the bubbles to cross a threshold into uncontrolled growth. Also, bubbles stabilized by mechanical structures will be destroyed if outside influences bring them below a critical small size. The in vivo behavior of different kinds of stabilized bubbles can be compared by using plots of bubble radius as a function of forces that affect diffusion of gases in or out of the bubble. The two ends of the plot are the limits for unstabilized growth and destruction; these and the curve's slope predict the bubble's practical usefulness for ultrasonic imaging or O_2 carriage to tissues.

bubble nuclei; cavitation; decompression sickness; surfactants; surface-active films; ultrasonic imaging

THERE ARE SEVERAL REASONS for interest in the behavior of small, stabilized gas cavities (bubbles) inside the human body. Microbubbles are being developed for enhancement of ultrasonic contrast of blood vessels and other body structures (5, 9, 13, 19, 20, 22, 30, 31). Some of these bubbles are small enough to traverse capillary beds and are stabilized by mechanisms that cause them to persist much longer than a simple bubble of air (23). Also, if microbubbles are permeable to gases, they could carry appreciable amounts of O_2 from lungs to tissues; it has been proposed that microbubbles could serve as a substitute for blood hemoglobin (4, 24). Furthermore, if stabilized bubbles are analogs of the micronuclei that may be the precursors of decompression sickness bubbles (18, 34) and the initiation sites for damaging cavitation in an ultrasonic field (2), their behavior is of interest in diving safety and medical uses of ultrasound. In all these cases, the way that the stabilized microbubbles respond to environmental changes is extremely important. If the change causes the microbubbles to become unstabilized, they can cease to exist or can grow into large, damaging bubbles.

Because pressure due to surface tension is a function of bubble size, it is obligatory for the stabilization mechanism to be a function of size as well (23). Two general classes of mechanisms can stabilize bubbles. First, slowly permeating gases (13) remain for relatively long times in the bubbles, while other more rapidly permeating gases diffuse in or out according to their concentrations in the environment (22, 23); total pressure inside is greater than that outside because of pressure due to surface tension. Second, structures at the gas-liquid interface can serve as stabilizers; examples are surface-active films (30), surface-active protein that may be denatured (19, 31), and gelatin (5). We have shown that, despite the differences between the two classes of stabilizing mechanisms, slowly permeating gases and structural stabilizers can be characterized by similar mathematical expressions (23).

The specific objectives of the present paper are to provide two extensions to our previously published theoretical treatments (4, 22–24): *1*) to include the idea that there are upper and lower size limits to stabilized bubbles and *2*) to consider how bubbles stabilized by various mechanisms can be compared. The crucial aspect of a structural stabilizer is that it must produce a negative pressure inside the bubble to counter the tendency for outward diffusion of the gases inside, especially to counter the strong positive internal pressure due to surface tension when bubbles are small. The theory presented below, couched in a mathematical framework, encompasses this fact and other basic facts that are valid for any stabilized bubble. We present examples to show how bubbles stabilized by different kinds of mechanisms may behave.

THEORY AND METHODS

In recent publications (4, 22–24), prediction of the behavior of stabilized microbubbles in blood depended on an important basic assumption: that the size of stabilized bubbles can vary in response to changes in the bubbles' surroundings; stabilization does not imply a fixed size or rigid structure. This assumption is supported by the observation that the ultrasonic signal from a bubble stabilized by an albumin coating decreased when pressure was applied and then returned to the initial level when pressure was released (15). For present purposes, we add another assumption: that the stabilizing mechanism may fail at some small size or rupture due to overexpansion. For most examples, we drew inspiration from surface films or surfactant monolayers, a specific type of

structural stabilizer. Other structural stabilizers will be analogous to surface films in that they counter surface tension but may differ in particulars.

An important related assumption is that the stabilized bubbles are permeable to diffusion of gases, so that diffusive exchanges will occur when there are gas partial pressure differences between inside and outside. The concept that gases diffuse in or out to change the contained volume when stabilized bubbles vary in size contrasts with the idea put forward by Yount and co-workers (32) that stabilized bubbles become impermeable when they are very small. It seems unlikely that a single layer of molecules, particularly if they are largely lipid in makeup, could prevent gas diffusion, even if densely packed. A monolayer could conceivably block water diffusion into the bubble and may slow permeation of some gases (3), but gases with high lipid solubility would have their diffusion enhanced by a lipid monolayer. Stabilized bubbles with multiple layers have been described (20), but if the layers are mainly lipid, permeability may not be appreciably affected.

We take advantage of a simplifying assumption so that we can use radius to characterize size: that stabilized bubbles always remain spherical. This is probably not valid for at least some kinds of bubbles; e.g., bubbles stabilized by shells of denatured protein are said to change shape when small (7), and bubbles stabilized by surfactant have been observed to become nonspherical when the surfactant molecules are forced close to each other (10). The assumption of sphericity and other simplifications mean that the results of our calculations are approximate; this does not detract from our goal of exploring the basic characteristics of stabilized bubbles.

The partial pressures of gases inside a bubble are influenced by hydrostatic pressures (23). The well-known Laplace-Young equation gives the hydrostatic pressure (P) exerted by surface tension on the contents of a spherical bubble

$$P_\gamma = \frac{2\gamma}{R} \qquad (1)$$

where R is bubble radius.

Glossary

β	Exponent defined by *Eq. 2*, dimensionless
ΔP_{abs}	Pressure difference for bubble absorption, kPa
γ	Surface tension, 50 dyn/cm = 50 kPa·μm
π	Constant, ~3.1416
Π	Reduction of surface tension due to a surface-active film, dyn/cm
A	Area per stabilizer element on a bubble surface, μm^2
A_c	Minimal area per structural element before crushing occurs, μm^2
A_o	Actual area that a stabilizer element occupies on a bubble surface, μm^2
b	Constant, $2\pi k T/A_c$, kPa·μm
c	Scaling constant for pressure exerted by an elastic sphere, kPa/μm
C_Γ	Constant that relates P_Γ to a function of bubble radius; units depend on the function
k	Boltzmann's constant, 1.3805×10^{-23} J/°K
n	Number of structural elements in a mechanical stabilizer
P_γ	Pressure generated by surface tension on a bubble, kPa
P_Γ	Pressure generated by a bubble stabilizer, kPa
P_z	Sum of all hydrostatic pressures and partial pressures that could affect diffusive exchanges of a bubble, other than those that depend on bubble radius, kPa
P_{z_c}	Pressure at the crushing radius R_c^*, kPa
P_{z_g}	Pressure at the critical growth radius R_g^*, kPa
R	Bubble radius, μm
R'	Unstressed radius of an elastic sphere, μm
R^*	Stable radius of a bubble, μm
R_c^*	Crushing radius of a bubble, μm
R_g^*	Critical growth radius of a bubble, μm
R_o	Asymptotic minimal radius of a bubble, μm
R_u^*	Stable radius of bubble when $P_z = 0$, μm
T	Temperature, °K

A stabilization mechanism exerts a counterpressure (P_Γ) against the tendency of surface tension and other forces to cause outward diffusion of the bubble's gaseous contents. A major point for this paper is that the behavior of a bubble is determined by behavior of P_Γ as a function of radius; each different stabilizer will have its own P_Γ function. To provide examples that have a quantitative basis, we relied on previous theory about bubbles stabilized by an ideal surfactant (23) for our starting point. We needed an expression that can account for the quantitatively different responses to stress that may occur with different kinds of stabilizing structures. We devised *Eq. 2* to satisfy this need; APPENDIX A shows the relation of *Eq. 2* to ideal surfactant films and bubbles of slowly permeating gas.

$$P_\Gamma = \frac{C_\Gamma}{R^{(\beta+1)}(R^2 - R_o^2)} \qquad (2)$$

According to *Eq. 2*, the pressure exerted by the stabilization mechanism is a ratio having a constant in the numerator and radius in the denominator, similar to the Laplace-Young equation, except that P_Γ involves the reciprocal of a function of radius instead of the simple reciprocal of radius. If the stabilizer is a surface-active film, the C_Γ constant is proportional to the number of molecules in the film. The R_o represents the minimal radius of the sphere made up of the aggregate of the elements of the mechanical stabilizer, and $(\beta + 1)$ is an arbitrary exponent. If β and R_o are both zero, *Eq. 2* is the formula for a simple, ideal "gaseous" surface-active film (23). Our introduction of the hypothetical β and R_o parameters allows us to anticipate the behaviors of real, nonideal surfactants that may be found in nature. Because the function of the stabilizer is to counter surface tension, the value of the right side of *Eq. 2* must be $>2\gamma/R$ when R is small; it follows that the value of β for a stabilized bubble can be any number more positive than -2.0. Our examples using *Eq. 2* are intended to portray some possibilities for real stabilizers; the purpose of the examples is to explore the general properties of different possible stabilizer mechanisms.

The hydrostatic pressures and partial pressures that affect the diffusive exchanges of a bubble can be categorized as positive absorptive pressures (ΔP_{abs}) that give a tendency for shrinkage or as negative absorptive pressures that give a tendency for growth. The sum of all pressures that relate to ΔP_{abs} is

$$\Delta P_{abs} = P_\gamma - P_\Gamma + P_z \qquad (3)$$

All terms in *Eq. 3* are in units of kPa (1 atm abs = 101.3 kPa); they are hydrostatic pressures or partial pressures. The P_γ and P_Γ terms are functions of bubble size, as seen by *Eqs. 1* and *2*. The term P_z symbolizes the sum of all influences that are independent of bubble size. Blood pressure is an example of a positive absorptive hydrostatic P_z. Another type of

positive P_z is the gas concentration difference due to the inherent unsaturation caused by O_2 metabolism, the so-called O_2 window (25), for a bubble in tissue or venous blood. The gas supersaturation that occurs in tissues of a diver who ascends from depth (27) is an example of a negative, size-independent concentration difference; the dissolved gas in the tissue is temporarily supersaturated, relative to the ambient pressure, so it tends to diffuse into a bubble.

Computations and plotting. We provide graphic examples developed using Microsoft QuickBasic on a Macintosh Classic computer. The plots assume surface tension to be 50 dyn/cm, a value reported for surface tension of blood (29).

RESULTS AND DISCUSSION

The three panels of Fig. 1 illustrate the effects of changes in P_z for one particular bubble. Figure 1*A* is the fundamental balance-of-forces diagram introduced in another publication (23). The uppermost dashed trace shows the absorptive pressure due to surface tension as a function of bubble radius. If unopposed, surface tension would have little effect when radius is large and, at small radii, would greatly elevate the hydrostatic pressure inside, causing outward diffusion of all constituent gases. The lowermost dashed trace in Fig. 1*A* shows P_Γ, the growth pressure exerted by a stabilization mechanism; if it were unopposed, the stabilizer would produce a growth tendency of about −50 kPa when radius is 2 μm and would exert very strong growth pressures at smaller radii.

The radius is stable where the Sum curve, the resultant of P_γ and P_Γ influences, crosses the axis for zero ΔPabs in Fig. 1*A* (at 2 μm). At the crossing, there is a positive slope so that if the bubble were slightly larger than its stable size, pressure due to surface tension would be greater than the negative pressure due to the stabilizer; there would be a positive pressure inside the bubble, which would cause gas inside to diffuse out until the bubble had shrunk down to the stable size. Conversely, if radius were between 1.5 and 2 μm in Fig. 1*A*, the bubble would grow to the stable radius. Every stabilized bubble, no matter what the mechanism, must have a positive slope on a balance-of-forces diagram, such as that illustrated in Fig. 1*A*. Stabilization requires that the P_Γ must be larger in magnitude than P_γ when radius is small. Within that constraint, P_Γ curves can have different shapes, as discussed below.

In addition to the point where the Sum curve crosses the axis for zero ΔPabs, two other important features in Fig. 1*A* are the point at which the Sum curve reaches a maximum (the square, which will be discussed just below in connection with Fig. 1*C*) and the left-hand end of the P_Γ curve. The ● represents the minimum size for the bubble's stabilization; we arbitrarily assign a minimum radius of 1.5 μm for this particular bubble; at smaller radii, the Sum curve does not exist because of failure of the stabilization mechanism. This is discussed further, in connection with Fig. 2*A*.

Figure 1*B* shows the effect of adding a third pressure, a P_z of +30 kPa (arrow), to the P_γ and P_Γ pressures of Fig. 1*A*. The addition moves the Sum curve up by 30 kPa over the entire range of radii. Comparison with Fig. 1*A* shows that the point where the Sum curve crosses the axis has moved to the left by ~0.3 μm. If a negative P_z had been added, the Sum curve would have been lowered instead of raised. Adding or subtracting various P_z values simply translates the Sum curve up or down, and the □ at the maximum of the Sum curve will be at the same radius, no matter what the P_z. It is shown next that when the maximum of the Sum curve is brought below the axis for zero ΔPabs, the bubble cannot be stable; it grows irreversibly.

Irreversible growth. The three solid Sum curves on Fig. 1*C* show effects of three different P_z values. A negative P_z acts in the same direction as the stabilization mechanism; both tend to cause growth. When P_z is negative enough to bring the maximum of the Sum curve below the axis for zero ΔPabs, a previously stabilized bubble grows into a relatively large, unstabi-

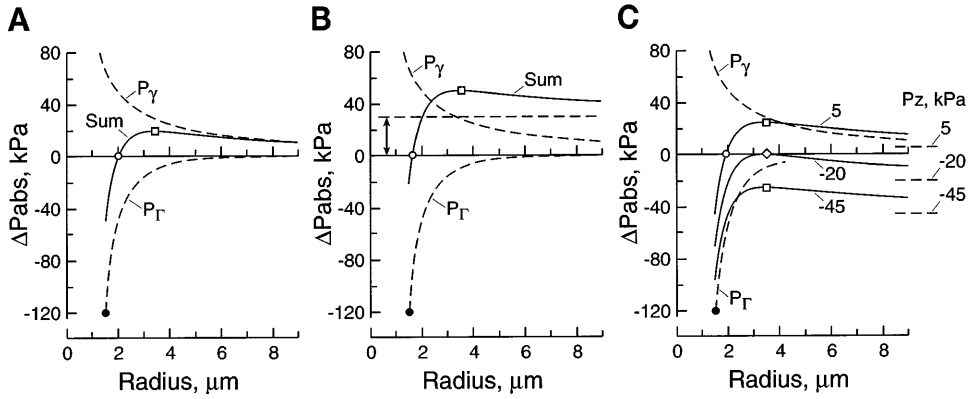

Fig. 1. Fundamentals of pressure difference for bubble absorption: (ΔPabs)-vs.-radius plots for 1 particular stabilized bubble. Dashed curves of pressure generated by surface tension on a bubble (P_γ) and pressure generated by a bubble stabilizer (P_Γ) are the same in *A*-*C* (P_γ curve drawn from *Eq. 1*, P_Γ curve from *Eq. 2* for $C_\Gamma = 400$ kPa·μm^3 with $\beta = 0$ and $R_o = 0$). *A*: curve labeled Sum (from *Eq. 3*) is the resultant of 2 oppositely acting pressures caused by surface tension and by stabilizer. ○, Stable radius; ●, point where stabilization mechanism fails; □, maximum of Sum curve. *B*: addition of a size-independent absorptive influence (horizontal dashed trace) moves Sum curve upward from where it was in *A* and decreases stable radius. *C*: 3 different Sum curves correspond to different P_z values (dashed horizontal line segments). ◇, "Critical growth" point where, because of a P_z of −20 kPa, bubble is on the verge of growing irreversibly. See *Glossary* for other definitions.

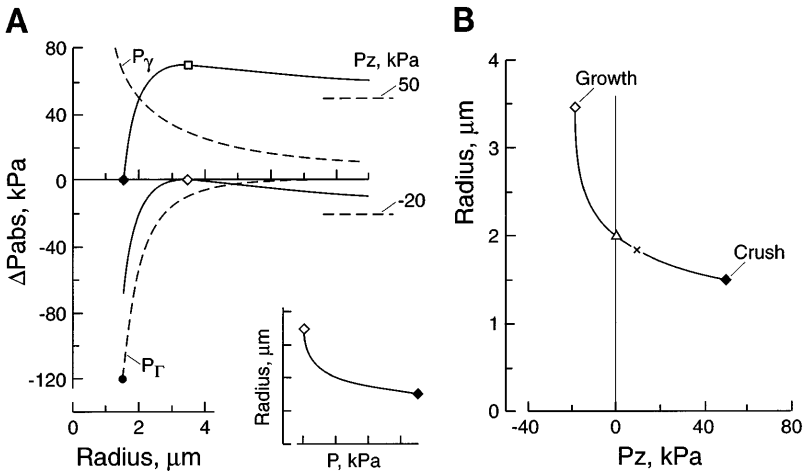

Fig. 2. Stability range for particular bubble that was shown in Fig. 1*A*. Solid traces show Sum curves for limiting possibilities. ◆, crushing radius; note that it is directly above ● on P_Γ curve; ◇, critical growth radius. *Inset*: counterclockwise rotation of either of solid curves of *panel A* gives a plot of radius vs. pressure. *B*: information from *panel A* replotted on a radius-vs.-P_z plot, with added points for unstressed radius (△) and for a bubble in venous blood (x).

lized bubble that can do damage in the body, as in decompression sickness (21, 27). For the curve with P_z of −45 kPa in Fig. 1*C*, there is no stable radius so the bubble grows irreversibly at all radii. The stabilized bubble with P_z of −20 kPa has a unique point (◇); P_z for that point is the critical P_z for irreversible growth, P_{z_g}. When a bubble is located at that point, the bubble would grow if, by chance, P_z became a little more negative or the radius increased a little. When the critical growth pressure is exceeded, the rate of growth that occurs increases as size increases because of the negative slope of the Sum curve to the right of the curve's maximum. As outlined before (21), when a small bubble is in an environment that fosters growth, there is a positive-feedback loop, whereby increased radius due to growth causes decrease of pressure due to surface tension, which encourages further growth. There is also a positive-feedback loop involving surface area of the bubble; as gases diffuse into the bubble, surface area increases, which, in turn, increases the amount diffusing under a particular gas concentration gradient.

Crushing. A bubble stabilized by a mechanical structure can be expected to behave in a discontinuous manner at small radii; a strong positive P_z may cause the bubble to reach its minimum size, beyond which it changes drastically or ceases to exist. Items in support of this possibility are the idea that micronuclei, the putative precursors of decompression-sickness bubbles, can be inactivated or "crushed" by high pressure (26); observations of "buckling" or "crumbling" of surface-active films (Ref. 1, p. 115; Ref. 17); observations of fissioning of bubbles into several smaller bubbles (33); and irreversible loss of ultrasonic signal from several types of microbubble contrast agents when pressure is applied to them (28).

The ● in Fig. 1*A* showed the radius and pressure combination at which the bubble's stabilization mechanism fails. We envision that there will be failure of the stabilizing molecules in most kinds of mechanical structures; we call the limiting small size the "critical crushing" radius. A P_z of +50 kPa will bring the Sum curve of the bubble depicted in Fig. 1 to 1.5 μm, the critical radius for bubble destruction or crushing; this is illustrated by the top solid curve in Fig. 2*A*.

When there is no longer a stabilization mechanism because of crushing, we envision that the bubble's gas contents rapidly diffuse out under the influence of surface tension. Hyldegaard et al. (12) observed that once a bubble in animal tissues had disappeared, application of growth influences did not make it reappear. On the other hand, Liebermann (14) observed that a residue left after apparent disappearance of free, unstabilized bubbles in water gave rise to new bubbles if the liquid was decompressed; this suggests that some sort of stabilized micronuclei remained in the residue. Bubbles stabilized by slowly permeating gas (13) may be an exception to the idea that all bubbles can be crushed; if the gas does not change phase to a liquid, such bubbles would not be expected to fail cataclysmically but will be absorbed more rapidly when P_z is large.

Limits to stabilization. A P_z of −20 kPa brought the Sum curve for the particular bubble shown in Figs. 1 and 2 to one limit of stability, where the bubble would grow irreversibly (lower solid curve in Fig. 2*A*) and addition of a sufficiently large positive P_z (+50 kPa) moved the Sum curve up to the critical point where crushing would occur (top solid curve in Fig. 2*A*). The Sum curves for all possible stabilized sizes must lie between the two solid curves shown in Fig. 2*A*. Because the two curves in Fig. 2*A* are for the same bubble, which has a particular C_Γ, they are identical except that they are translated vertically from each other by differences in P_z. The *inset* shows either of the two solid Sum curves of Fig. 2*A* rotated 90° counterclockwise. Such a pressure-vs.-radius display is analogous to stress-vs.-strain diagrams for other materials. The display is made practical by using P_z for the pressure axis, as we have done in Fig. 2*B*.

Radius vs. P_z. Figure 2*B* shows all possible radius-vs.-P_z combinations for the particular bubble under consideration when it is in a stable condition. When P_z is zero, the radius is unstressed (at radius = 2 μm). When stress due to P_z is positive, radius declines with increasing P_z until the bubble reaches the positive pressure that causes crushing (at radius = 1.5 μm).

When stress due to P_z is negative, radius enlarges until the bubble reaches the negative pressure that causes unstabilized growth (at radius = 3.4 μm). Compliance of the bubble can be defined as the slope of the radius-vs.-P_z curve. Clearly, compliance is specific to the prevailing P_z. The changes of radius in Fig. 2*B* correspond to large changes of volume because of the cubic relation between radius and volume: the volume at the critical growth radius is 12 times greater than the volume at the critical crushing radius. APPENDIX B presents the mathematical relationships implicit in the type of curve shown in Fig. 2*B* for one particular kind of structural stabilizer.

In traversing the circulatory system, a stabilized bubble will encounter various P_z values (23). In mixed venous blood, the sum of partial pressures of dissolved gases is less than atmospheric pressure because of removal of O_2 by metabolism. In an air-breathing subject, the value of this inherent unsaturation is ~7 kPa (25); the corresponding point on Fig. 2*B* is shown by x. In O_2 breathing, the inherent unsaturation is much higher, such as 89 kPa (24); this falls beyond the ◆ on the curve in Fig. 2*B*. If subjected to P_z of 89 kPa, the particular bubble illustrated here would be crushed in the tissue capillaries or venous blood. To have persistent bubbles that can recirculate in a person breathing pure O_2, it would be necessary to have a bubble that is stabilized by a mechanism with a stronger resistance to crushing.

Note that because displays such as Fig. 2*B* are for the condition of stability, the bubble is in diffusive equilibrium with its surroundings for all points on the curve. After a rapid change in the environment, there will be a transient phase in which the bubble leaves the radius-vs.-P_z curve. Diffusive readjustment of contents will bring the bubble back to rest on the curve.

Varieties of stabilizers. Figures 1 and 2 show how a single bubble with a particular stabilization mechanism behaves as environmental conditions change. In what follows, we focus on distinguishing between different stabilization mechanisms. We hope to gain insights into possibilities for various kinds of real bubbles by simulating the behaviors of hypothetical bubbles having various characteristics; to do so, we vary the parameters in *Eq. 2*.

Figure 3*A*, drawn for the specific kind of stabilizer that is dealt with in APPENDIX B, shows that larger C_Γ moves the stabilizer curve to the right and down. Figure 3*B* shows that larger C_Γ gives larger bubbles that require less negative P_z for unstabilized growth and less positive P_z for crushing; in Fig. 3*B*, larger bubbles are more fragile than small bubbles: they are less resistant both to growth and to crushing. Higher C_Γ gives a steeper slope at $P_z = 0$.

The nature of the stabilization mechanism determines the shape of a curve of stabilizer pressure as a function of bubble size. Our examples so far have used *Eq. 2* with a (β +1) exponent of 1.0 and R_o asymptote of zero; these choices approximate the behavior of a bubble stabilized by either a slowly permeating gas or by a "gaseous" type of surfactant film (23). We presume

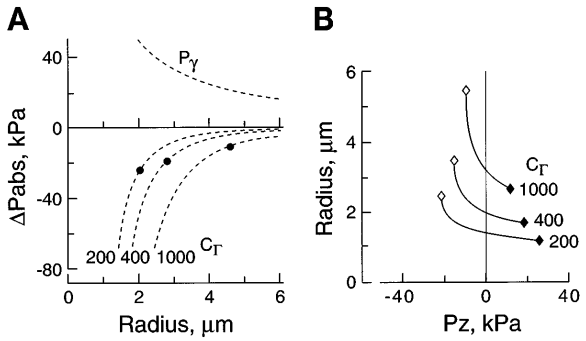

Fig. 3. Consequences of variations of constant relating P_Γ to a function of bubble radius (C_Γ); dashed curves were drawn from *Eq. 2* with $\beta = 0$ and $R_o = 0$. *A*: location of stabilizer curves for different values of C_Γ. ●, Crush points for an arbitrary choice of 140 kPa·μm for *b* in *Eq. B11*. *B*: radius-vs.-P_z curves for the 3 cases of *panel A*. See *Glossary* for other definitions.

that we can approximate curves for other types of surfactants or mechanical structures by varying the β exponent or the R_o asymptote; a few examples are presented in Fig. 4.

Figure 4, *A* and *B*, displays effects of alterations in the value of the β parameter to simulate variations in the mechanical properties of stabilizers. When β is large, the P_Γ curves are steeper (Fig. 4*A*), the radius-vs.-P_z curves are more horizontal where they cross the axis for zero P_z (Fig. 4*B*), and the bubbles are more resistant to unstabilized growth (◇ in Fig. 4*B*). We cannot anticipate the effect of different β values on the crushing phenomenon, so we arbitrarily chose to set the crushing point at a constant P_{z_c}. However, it may be

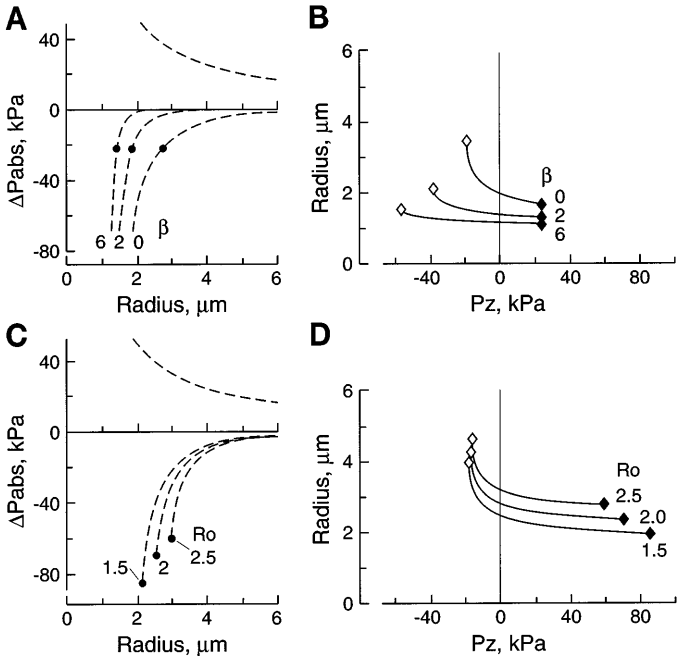

Fig. 4. Variations of characteristics of structural stabilizers. As in Fig. 3, stabilizer curves are at *left*, radii as a function of P_z are at *right*. *A* and *B*: variation of exponent β in *Eq. 2* (with C_Γ = 400 kPa·μm^3, $R_o = 0$; crushing arbitrarily set at P_z = 23.4 kPa). *C* and *D*: variation of R_o in *Eq. 2* [with C_Γ = 400, $\beta = 0$, crushing occurs when $(R_c^{*2} - R_o^2)$ is less than a certain value, arbitrarily set at 1.5 μm^2]. See *Glossary* for other definitions.

that the steeper curves in Fig. 4*A* are also more resistant to crushing; if so, the curves for larger β values should have the crush point at greater negative ΔPabs in Fig. 4*A* and greater positive P_z in Fig. 4*B*.

Because R_o characterizes the aggregate surface area of elements of the mechanical stabilizer, larger R_o indicates larger elements. An increase in R_o moves the asymptotes to the right and causes divergence of the stabilizer curves from each other at negative ΔPabs values (Fig. 4*C*). The consequences are that there is little variation of the P_z for unstabilized growth but there is variation in the crushing P_z (Fig. 4*D*). Bubbles with large R_o are less resistant to crushing.

Note that the kinds of diagrams shown in Figs. 3 and 4 may be crude approximations for real bubbles. The P_Γ curves may not fall smoothly to the left as shown in Figs. 3*A*, 4*A*, and 4*C* if there are changes in the state of the material in the structure. For example, if a surfactant film goes from "gaseous" to "liquid" to "solid" states (Ref. 1, p. 129–133), each state may have its own smooth curve, which is joined to the curve for the next state at a transition point. Other complexities are likely. For example, a bubble that collapses like a football bladder when its volume decreases would have different radii in different aspects, and one of the radii would change much more than others when volume decreases.

Coherent elements. Some bubbles may be stabilized by elements or molecules that tend to cohere to each other, such as denatured proteins (7, 15, 19, 28, 31). Such materials can be expected to exhibit the property of elasticity, which would result in a ΔPabs-vs.-radius plot that rises without leveling off, as depicted in Fig. 5*A*. As in Figs. 1–4, the Sum curve is the sum of contributions from the P_γ curve and the P_Γ curve. For this case, the P_Γ curve was drawn by a formula inspired by properties of elastic sheets: $P_\Gamma = c\,[R - (R'^2/R)]$. This formula incorporates the idea that force per unit length exerted by an elastic sheet that covers a sphere is proportional to change of area from an unstressed area (with radius = R') and was derived by analogy with *Eqs. A1-A6* in APPENDIX A. For Fig. 5, we arbitrarily assigned the scaling constant c to be 10 kPa/μm and R' to be 4 μm. Although the Sum curve has no maximum, irreversible growth can occur by a different mechanism. The discontinuity on the right end of the P_Γ curve of the elastic, coherent material in Fig. 5*A* represents failure of the stabilizer because of excessive stretch, analogous to explosion of a balloon when it is overinflated. In Fig. 5*B*, an added P_z of −50 kPa lowers every point on the Sum curve so that the stable radius is at the point of the discontinuity in the stabilizer curve. After the stabilization structure ruptures and no longer provides a counterpressure, there are only two forces acting on the gases in the bubble: surface tension is small because the size of the bubble is large, and the negative P_z that was used to induce the present state is relatively large. The sum of these puts the bubble in the growth region, so it grows (arrow in Fig. 5*C*).

Figure 5*D* is a plot of radius as a function of P_z for the elastic stabilizer, analogous to Fig. 2*B*. The ◆ on the *left*

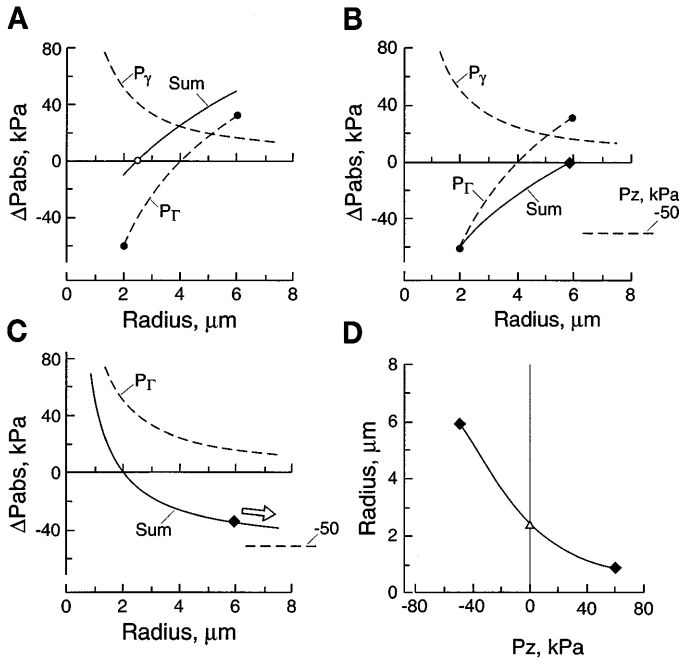

Fig. 5. Behavior of a bubble stabilized by an elastic material. *A*: Sum curve proceeds upward in absorptive region at *right* without a maximum. ○, Stable radius. Stabilization may fail due to crushing (*left* ●) or overexpansion (*right* ●). *B*: addition of a large negative P_z lowers the sum curve and increases stable radius to where it is overstretched and destroyed (◆). *C*: after stabilizer disappears, bubble grows irreversibly (arrow). *D*: P_z-vs.-radius plot of bubble shown on *panels A-C*. △, Unstressed radius; ◆, rupture points; compliance is more uniform over range of P_z than with Figs. 3 and 4.

represents the point at which the structure ruptures, producing an unstabilized bubble that grows. We envision that this sort of elastic membrane will crush or rupture at high positive pressures in the same way as a surfactant-stabilized bubble, so that it ceases to serve as a stabilizer at some small radius (◆ on *right*).

Applications of radius-vs.-P_z curves. Knowledge of how bubbles behave when they are stabilized by a particular mechanism would allow practitioners to choose the bubble with appropriate characteristics for a particular purpose. Also, specific characteristics can be sought in the formulation of bubbles by new techniques or by the use of new materials. It might be desirable, for example, to have bubbles that would not be crushed at all under physiological conditions or, alternatively, an application might call for bubbles that would be crushed by arterial blood pressure. A radius-vs.-P_z curve conveniently summarizes the characteristics of different kinds of stabilized bubbles; the critical growth radius, the unstressed radius, the crushing radius, and the bubble's compliance all appear on one simple graph. Data to characterize a particular bubble on a radius-vs.-P_z curve could be obtained by microscopic observations of it during slow changes of external pressure while dissolved gases in the liquid environment are controlled.

We next cite three cases where distinguishing between different types of bubbles may be desirable. First, if bubbles are used to augment O_2 carriage by blood (4), the amount of O_2 that is unloaded at a

particular partial pressure depends heavily on the bubble's tendency to change size as well as on the local P_{O_2} (24). Therefore, a highly compliant bubble is desirable if one wants to unload large amounts of O_2 in tissue at a given partial pressure. The curves in Fig. 3*B* indicate that bubbles with larger C_Γ generally exhibit greater compliance (change of radius per change of pressure). In contrast, noncompliant bubbles, such as those with higher β exponent illustrated in Figs. 4*A* and 4*B*, would be less effective in O_2 delivery.

Second, it remains to be seen which stabilizer characteristics give the best signal when bubbles are used for ultrasonic contrast (16, 35): large elements, many elements, or large compliance. In some circumstances, the ultrasonic signal due to a bubble is proportional to the sixth power of radius (35), so stabilizing mechanisms that give rise to large bubbles offer far more enhancement of a given signal than mechanisms that make for smaller bubbles.

The third case concerns the idea that the precursors of decompression-sickness bubbles are permanent or semipermanent small bubbles or gaseous "micronuclei" (11, 21, 34) stabilized by structures of the kind discussed in this paper. If so, *Eqs. B8* and *B11* indicate that large micronuclei are both more easily destroyed by crushing and more easily transformed into bubbles. Exposure of a diver to high environmental pressure is thought to crush micronuclei (26). If so, the crushing would delete some of the population of micronuclei, so there would be fewer available to be forced into irreversible growth to cause damaging bubbles by the subsequent decompression (18). Furthermore, it would be desirable to determine the characteristics of the stabilizing mechanisms of decompression-sickness precursors; perhaps it will be possible to develop techniques to interfere with their transformation into damaging bubbles.

APPENDIX A

Relationship of Eq. 2 to Surface Films

Equation A1 describes the behavior of various nonideal gaseous surfactants on a planar surface, such as on a Langmuir trough (Ref. 6, p. 228)

$$\Pi(A - A_o) = nk\mathrm{T} \qquad (A1)$$

Total area A that is occupied by the surface-active film has a minimum, A_o, and the reduction of surface tension due to the film, Π, is related to the number n of molecules or elements in the film. Because Π is the difference of surface tension between pure solvent and solvent containing the surfactant (Ref. 6, p. 218), it has the nature of a surface tension, so the Laplace-Young equation can characterize the counterpressure on a spherical bubble due to the surfactant

$$P_\Gamma = \frac{2\Pi}{R} \qquad (A2)$$

Substitution with *Eq. A1* gives

$$P_\Gamma = \frac{2nk\mathrm{T}}{R(A - A_o)} \qquad (A3)$$

Converting the area terms to radius terms yields

$$P_\Gamma = \frac{2nk\mathrm{T}}{4\pi R(R^2 - R_o^2)} \qquad (A4)$$

where R is the radius of the bubble, and R_o is the minimal radius.

We group constants in *Eq. A4* into a single constant C_Γ

$$C_\Gamma = \frac{nk\mathrm{T}}{2\pi} \qquad (A5)$$

Thus the C_Γ constant is proportional to the number of stabilizer elements in the interface (23).

Substitution of the C_Γ constant into *Eq. A4* yields

$$P_\Gamma = \frac{C_\Gamma}{R(R^2 - R_o^2)} \qquad (A6)$$

To allow approximation of some types of stabilizers that differ in properties from the film characterized by *Eq. A1*, we broaden *Eq. A6* by arbitrarily raising one of the R terms to a power

$$P_\Gamma = \frac{C_\Gamma}{R^{(\beta+1)}(R^2 - R_o^2)} \qquad (2)$$

If β is 0, *Eq. 2* equals *Eq. A6*. If both β and R_o are zero, *Eq. 2* is appropriate for bubbles stabilized by a slowly permeating gas (23) and by the ideal surfactant discussed in APPENDIX B.

APPENDIX B

Mathematical Characterization of Stable Radii

In what follows, we develop equations that are applicable to bubbles stabilized by ideal gaseous surfactants and by slowly permeating gases (23) and are approximations for bubbles stabilized by other kinds of surfactant. This simplified case is convenient for mathematical manipulations; it uses a simplified form of *Eq. 2* in which both R_o and β are zero

$$P_\Gamma = \frac{C_\Gamma}{R^3} \qquad (B1)$$

By using *Eq. 1* and *Eq. B1*, *Eq. 3* can be written as a function of radius

$$\Delta\mathrm{Pabs} = \frac{2\gamma}{R} - \frac{C_\Gamma}{R^3} + P_z \qquad (B2)$$

When a bubble is at a stable radius R^*, ΔPabs = 0, so there is no net diffusion of gas between the bubble and its surroundings

$$P_z = \frac{C_\Gamma}{R^{*3}} - \frac{2\gamma}{R^*} \qquad (B3)$$

Unstressed radius. For one specific stable radius, there is no size-independent influence on the bubble; that is, $P_z = 0$. We refer to this as the "unstressed radius." Set P_z to zero in *Eq. B3*

$$R_u^* = \left(\frac{C_\Gamma}{2\gamma}\right)^{0.5} \qquad (B4)$$

It is seen that R_u^* is a function of the ratio of the stabilization

constant to the surface tension; examples of unstressed radii are seen at the intersections of the curves with the zero P_z axis in Figs. 2*B* and 3*B*.

Critical radius for irreversible growth. We next amplify on the contention, illustrated in Fig. 1*C* and 2*A*, that the maximum of a Sum curve on a ΔPabs-vs.-radius plot is associated with an upper limit to the radius for a stabilized bubble. The limiting large size is brought about when addition of a strong growth pressure (negative P_z) brings the maximum of the Sum curve to the zero ΔPabs axis. The smallest pressure at which the bubble is forced from a stable state into a state of unstable growth can be called the "critical growth pressure" (P_{z_g}), and the size of the bubble at that pressure can be called the "critical growth radius" (R^*_g).

The maximum of the Sum curve is found by equating the first derivative of ΔPabs as a function of R (*Eq. B2*) to zero

$$\frac{\mathrm{d}(\Delta\mathrm{Pabs})}{\mathrm{d}R} = \frac{2\gamma}{R^2} - \frac{3C_\Gamma}{R^4} = 0 \qquad (B5)$$

The critical growth radius is the radius at which the bubble is both stable (ΔPabs = 0) and at the maximum defined by *Eq. B5*

$$R^*_g = \left(\frac{3C_\Gamma}{2\gamma}\right)^{0.5} \qquad (B6)$$

As with R^*_u in *Eq. B4*, R^*_g is a function of the ratio of the stabilization constant to the surface tension. Combination of *Eqs. B4* and *B6* shows that the growth radius is $\sqrt{3}$ times larger than the unstressed radius.

Putting *Eq. B6* into *Eq. B3* yields an expression for critical growth pressure as a function of C_Γ

$$P_{z_g} = -\frac{4}{3}\left(\frac{2\gamma^3}{3C_\Gamma}\right)^{0.5} \qquad (B7)$$

According to *Eq. B7*, bubbles with large C_Γ require less P_z to cause irreversible growth than bubbles with small C_Γ.

The dependence of critical growth radius on imposed P_z, seen as ◇ in Fig. 3*B*, is given by solving *Eq. B6* for C_Γ and putting the result into *Eq. B3*

$$P_{z_g} = -\frac{4\gamma}{3R^*_g} \qquad (B8)$$

It is seen that *Eq. B8* is analogous to the Laplace-Young equation: a pressure is inversely proportional to the first power of radius. Consonant with *Eq. B8*, the points for transition to irreversible growth (◇) in the cases shown in Figs. 3*B*, 4*B*, and 4*D* trace out paths in which P_z to cause growth is inversely related to radius.

Critical radius for crushing. We assume that a spherical, structurally stabilized bubble is crushed when its surface area is reduced to some particular small area at which the structural elements are pressed together maximally

$$4\pi R^{*2}_c = nA_c \qquad (B9)$$

where A_c is minimal area per structural element and n is number of structural elements. The maximal pressure that can be withstood is the "crushing pressure." An example of crushing behavior is the collapse of surface-active films at some maximal surface pressure (Ref. 1, p. 115) because the area approaches the minimal surface area of the aggregate of the molecules that comprise the film. Possibilities for action of the high surface pressure in a surfactant film include tearing of the stabilization mechanism, forcing part of the film to ride up over other parts, making the film transform into a "solid-phase" film that is no longer as compressible and cannot reexpand when absorptive forces are relieved (8), or "squeezing" some of the molecules of the surfactant out of the film (17).

The relation between C_Γ and the crushing radius is found by putting *Eqs. A5* and *B9* together and combining constants

$$C_\Gamma = \frac{2kTR^{*2}_c}{A_c} = bR^{*2}_c \qquad (B10)$$

The A_c in *Eq. B10* defines the left-hand end of the P_Γ curves of Figs. 3*A*, 4*A*, and 4*C*; we made arbitrary choices for A_c to give the crushing radii for the Figs. 3*A*, 4*A*, and 4*C*.

We enter *Eq. B10* into *Eq. B3* to characterize the pattern of the filled diamonds in Fig. 3*B*

$$P_{z_c} = \frac{b - 2\gamma}{R^*_c} \qquad (B11)$$

According to *Eq. B11*, the P_z to cause crushing is a pressure equal to b/R^*_c minus the surface tension pressure at that radius ($2\gamma/R^*_c$). The absorptive force of surface tension aids the external P_{z_c} in the crushing phenomenon. As predicted by *Eq. B11*, the crushing points trace out paths inversely related to radius in Figs. 3*B* and 4*D* .

Recombination of variables shows that P_{z_c} is inversely proportional to the square root of C_Γ

$$P_{z_c} = (b - 2\gamma)\left(\frac{b}{C_\Gamma}\right)^{0.5} \qquad (B12)$$

The relations developed above were used to produce the diagrams in Figs. 1–3 and are in accord with the trends of the curves in Fig. 4, but do not apply to Fig. 5.

We are greatly indebted to Mark E. Burkard for insightful suggestions and criticisms.

Address for reprint requests: H. D. Van Liew, Dept. of Physiology, 25 Sherman Annex, State Univ. of New York at Buffalo, SUNY, Buffalo, NY 14214.

Received 3 May 1996; accepted in final form 11 February 1997.

REFERENCES

1. **Adamson, A. W.** *Physical Chemistry of Surfaces* (3rd ed.). New York: Wiley, 1976.
2. **Apfel, R. E., and C. K. Holland.** Gauging the likelihood of cavitation from short-pulse, low-duty cycle diagnostic ultrasound. *Ultrasound Med. Biol.* 17: 179–185, 1991.
3. **Blank, M.** The permeability of monolayers to several gases. In: *Retardation of Evaporation by Monolayers*, edited by V. K. La Mer. New York: Academic, 1962, p. 75–95.
4. **Burkard, M. E., and H. D. Van Liew.** Oxygen transport to tissue by persistent bubbles: theory and simulations. *J. Appl. Physiol.* 77: 2874–2878, 1994.
5. **Carroll, B. A., R. J. Turner, E. G. Tickner, D. B. Boyle, and S. W. Young.** Gelatin encapsulated nitrogen microbubbles as ultrasonic contrast agents. *Invest. Radiol.* 15: 260–266, 1980.
6. **Davies, J. T., and E. K. Rideal.** *Interfacial Phenomena* (2nd ed.). New York: Academic, 1963.
7. **De Jong, N., F. J. Ten Cate, W. B. Vletter, and J. R. T. C. Roelandt.** Quantification of transpulmonary echocontrast effects. *Ultrasound Med. Biol.* 19: 279–288, 1993.
8. **Goerke, J., and J. A. Clements.** Alveolar surface tension and lung surfactant. In: *Handbook of Physiology. The Respiratory System. Mechanics of Breathing.* Bethesda, MD: Am. Physiol. Soc., 1986, sect. 3, vol. III, pt. 1, chapt. 16, p. 247–261.

9. **Goldberg, B. B., J.-B. Liu, and F. Forsberg.** Ultrasound contrast agents: a review. *Ultrasound Med. Biol.* 20: 319–333, 1994.
10. **Hall, S. B., M. S. Bermel, Y. T. Ko, H. J. Palmer, G. Enhorning, and R. H. Notter.** Approximations in the measurement of surface tension on the oscillating bubble surfactometer. *J. Appl. Physiol.* 75: 468–477, 1993.
11. **Hills, B. A.** Release of surfactant and a myelin proteolipid apoprotein in spinal tissue by decompression. *Undersea Hyperb. Med*. 21: 95–102, 1994.
12. **Hyldegaard, O., M. Møller, and J. Madsen.** Effect of He-0_2, O_2, and N_2O-O_2 breathing on injected bubbles in spinal white matter. *Undersea Biomed. Res.* 18: 361–371, 1991.
13. **Kenny, A., D. J. Sahn, T. Shiota, A. Passafini, G. Pantely, A. Arai, M. Jones, S. Ge, I. Yamada, and M. D. Reller.** A new phase shift echo contrast agent: EchoGen (Sonus Pharmaceuticals) becomes a gas in blood to produce left heart and quantifiable myocardial contrast after venous injection. Studies in sheep and monkeys (Abstract). *J. Am. Coll. Cardiol.* 21: 450A, 1994.
14. **Liebermann, L.** Air bubbles in water. *J. Appl. Phys.* 28: 205–211, 1957.
15. **Mor-Avi, V., S. G. Shroff, K. A. Robinson, A. F. Ng, B. P. Cholley, R. H. Marcus, and R. M. Lang.** Effects of left ventricular pressure on sonicated albumin microbubbles: evaluation using an isolated rabbit heart model. *J. Am. Coll. Cardiol.* 24: 1779–1785, 1994.
16. **Ophir, J., and K. J. Parker.** Contrast agents in diagnostic ultrasound. *Ultrasound Med. Biol.* 15: 319–333, 1989.
17. **Otis, D. R., Jr., E. P. Ingenito, R. D. Kamm, and M. Johnson.** Dynamic surface tension of surfactant TA: experiments and theory. *J. Appl. Physiol.* 77: 2681–2688, 1994.
18. **Raychaudhuri, S., and H. D. Van Liew.** Mathematical analysis of the transformation of micronuclei into decompression sickness bubbles (Abstract). *Undersea Hyperb. Med*. 22S: 68, 1995.
19. **Ten Cate, F. J., P. Widimsky, J. H. Cornel, D. J. Waldstein, P. W. Serruys, and A. Waaler.** Intracoronary albunex. Its effects on left ventricular hemodynamics, function, and coronary sinus flow in humans. *Circulation* 88: 2123–2127, 1993.
20. **Unger, E., D.-K. Shen, T. Fritz, B. Kulik, P. Lund, G.-L. Wu, D. Yellowhair, R. Ramaswami, and T. Matsunaga.** Gas-filled lipid bilayers as ultrasound contrast agents. *Invest. Radiol.* 29: S134–S136, 1994.
21. **Van Liew, H. D.** Simulation of the dynamics of decompression sickness bubbles and the generation of new bubbles. *Undersea Biomed. Res.* 18: 333–345, 1991.
22. **Van Liew, H. D., and M. E. Burkard.** Behavior of bubbles of slowly permeating gas used for ultrasonic imaging contrast. *Invest. Radiol.* 30: 315–321, 1995.
23. **Van Liew, H. D., and M. E. Burkard.** Bubbles in circulating blood: stabilization and simulations of cyclic changes of size and content. *J. Appl. Physiol.* 79: 1379–1385, 1995.
24. **Van Liew, H. D., and M. E. Burkard.** Relationship of oxygen content to Po_2 for stabilized bubbles in the circulation: theory. *J. Appl. Physiol.* 81: 500–508, 1996.
25. **Van Liew, H. D., J. Conkin, and M. E. Burkard.** The oxygen window and decompression bubbles: estimates and significance. *Aviat. Space Environ. Med*. 64: 859–865, 1993.
26. **Vann, R. D., J. Grimstad, and C. H. Nielsen.** Evidence for gas nuclei in decompressed rats. *Undersea Biomed. Res.* 7: 107–112, 1980.
27. **Vann, R. D., and E. D. Thalmann.** Decompression physiology and practice. In: *The Physiology and Medicine of Diving* (4th ed.), edited by P. B. Bennett and D. H. Elliott. Philadelphia, PA: Saunders, 1993, p. 376–432.
28. **Vuille, C., M. Nidorf, R. L. Morrissey, J. B. Newell, A. E. Weyman, and M. H. Picard.** Effect of static pressure on the disappearance rate of specific echocardiographic contrast agents. *J. Am. Soc. Echocardiogr*. 7: 347–354, 1994.
29. **Walder, D. N.** Serum surface tension and its relation to the decompression sickness of aviators. *J. Physiol. (Lond.)* 548: 48P–49P, 1948.
30. **Wheatley, M., B. Schrope, and P. Shen.** Contrast agents for diagnostic ultrasound: development and evaluation of polymer-coated microbubbles. *Biomaterials* 11: 713–717, 1990.
31. **Wilson, B., K. K. Shung, B. Hete, H. Levene, and J. L. Barnhart.** A feasibility study on quantitative myocardial perfusion with Albunex, an ultrasonic contrast agent. *Ultrasound Med. Biol*. 19: 181–191, 1993.
32. **Yount, D. E.** Skins of varying permeability: a stabilization mechanism for gas cavitation nuclei. *J. Acoust. Soc. Am*. 65: 1429–1439, 1979.
33. **Yount, D. E.** A model for microbubble fission in surfactant solutions. *J. Colloid Interface Sci*. 91: 349–360, 1983.
34. **Yount, D. E., and R. H. Strauss.** Bubble formation in gelatin: a model for decompression sickness. *J. Appl. Phys.* 47: 5081–5089, 1976.
35. **Ziskin, M. C., A. Bonakdarpour, D. P. Weinstein, and P. R. Lynch.** Contrast agents for diagnostic ultrasound. *Invest. Radiol*. 7: 500–505, 1972.